2007

Ductile ultrafine-grained Ti-based alloys with high yield strength

Lai-Chang Zhang
IFW Dresden, laichang@uow.edu.au

Hai-Bo Lu
IFW Dresden, hlu@uow.edu.au

Christine Mickel
IFW Dresden

Jurgen Eckert
IFW Dresden

Publication Details

Zhang, L. Chang., Lu, H. Bo., Mickel, C. & Eckert, J. (2007). Ductile ultrafine-grained Ti-based alloys with high yield strength. Applied Physics Letters, 91 (5), 051906-1-051906-3.

Ductile ultrafine-grained Ti-based alloys with high yield strength

Lai-Chang Zhang[a)]
Institut für Komplexe Materialien, IFW Dresden, Postfach 27 01 16, D-01171 Dresden, Germany

Hai-Bo Lu and Christine Mickel
Institut für Metallische Werkstoffe, IFW Dresden, Postfach 27 01 16, D-01171 Dresden, Germany

Jürgen Eckert
Institut für Komplexe Materialien, IFW Dresden, Postfach 27 01 16, D-01171 Dresden, Germany

(Received 18 May 2007; accepted 5 July 2007; published online 31 July 2007)

The authors report on ductile ultrafine-grained $(Ti_{0.72}Fe_{0.28})_{100-x}Ta_x$ $(0 \leqslant x \leqslant 4)$ alloys with not only high fracture strength but simultaneously high yield strength exceeding 2000 MPa along with distinct plasticity, which are superior to high-strength Ti-based bulk metallic glasses and bimodal composites. All alloys mainly consist of β-Ti and FeTi solid solutions but display different microstructures. The alloys exhibit a high fracture strength >2500 MPa and a high yield strength >2000 MPa as well as large plasticity of ~5%–7.5%. The microstructure-property correlation of these ultrafine-grained alloys is discussed. © *2007 American Institute of Physics*.
[DOI: 10.1063/1.2766861]

Nowadays, the improvement of the strength and the room temperature plasticity of nano-/ultrafine-grained metallic materials has become a key topic in the development of advanced structural materials.[1,2] Compared with other metallic materials, titanium alloys are one of the best lightweight engineering materials for many industrial applications due to their excellent mechanical properties (yield strength ~1000 MPa and ductility ~10%) and good corrosion resistance.[3] Recently, Ti-based metallic glasses[4–13] and bimodal composites[14–20] have been developed with the aim to obtain high-strength Ti alloys. In the former case, they either contain the toxic constituent beryllium or have a low Ti concentration (≤50 at. %) as well as a limited size (<3 mm) if without Be, which will restrict their practical applications. The Be-free Ti-based bulk metallic glasses (BMGs) usually exhibit a high fracture strength exceeding ~2000 MPa but very limited plasticity (<0.5%).[4–7] The Be-containing Ti-based BMGs exhibit a larger plasticity of about 1%–5% but with lower fracture strength of ~1750 MPa.[8,9] However, their plasticity does not result from the glassy phase itself but is closely related to the amount of nanocrystals embedded in the glassy matrix.[21] On the other hand, the Ti-based bimodal composites display much higher fracture strength (~2000–2600 MPa) and larger plasticity (>2%) compared with the metallic glasses. For example, the $Ti_{60}Cu_{14}Ni_{22}Sn_4Nb_{10}$ alloy reaches a strength of 2400 MPa and 14.5% plastic strain,[14] and $Ti_{63.375}Fe_{34.125}Sn_{2.5}$ exhibits a strength of 2650 MPa and a plasticity of 12.5%.[17] However, the reported high fracture strength for the Ti-based bimodal composites is linked with pronounced strain hardening after yielding. Actually, they show a much lower yield strength (~1300–1800 MPa) compared with the Be-free Ti-based BMGs (~2000 MPa). Note that the yield strength is more important than the fracture strength for practical application of a material. Therefore, it would be desirable to further develop Ti-based alloys with high yield strength and not only high fracture strength similar as for Ti-based BMGs but with a plasticity similar to Ti-based bimodal composites.

In this letter, we report on the formation of ultrafine-grained (UFG) Ti–Fe–Ta alloys with a combination of mechanical properties superior to Ti-based BMGs and bimodal composites. The as-developed UFG Ti-based alloys exhibit not only a high fracture strength >2500 MPa but also a high yield strength >2000 MPa along with a distinct plasticity of 5%–7.5%.

Master alloys with nominal composition of $(Ti_{0.72}Fe_{0.28})_{100-x}Ta_x$ $(0 \leqslant x \leqslant 4)$ were prepared from elemental pieces with purity ≥99.99% by arc melting under a Ti-gettered argon atmosphere in a water-cooled copper crucible. Rods with 3 mm diameter were cast from the master alloy ingots into a copper mold under Ar atmosphere. The structural features of the cross section of the rods were examined by x-ray diffraction (XRD) using a Philips PW 1050 diffractometer with monochromated Co $K\alpha$ radiation. The microstructures of the cross-sectional surfaces were characterized using a JEOL JSM 6400 scanning electron microscopy (SEM) and a JEOL 2000FX transmission electron microscope (TEM) coupled with energy-dispersive x-ray analysis. The room temperature mechanical properties were evaluated by uniaxial compression tests in an Instron 8562 testing machine at a strain rate of 1.2×10^{-4} s^{-1}.

The XRD patterns of the as-cast alloys are shown in Fig. 1(a). All alloys mainly consist of body-centered-cubic (bcc) β-Ti and bcc FeTi solid solutions. The lattice parameters are $a_{\beta\text{-Ti}}$=0.3154, 0.3152, and 0.3163 nm and a_{FeTi} =0.2993, 0.2998, and 0.3001 nm for x=0, 2, and 4, respectively. The internal lattice strain of the β-Ti phase was calculated using the well-known Williamson-Hall method to be 0.57%, 0.81%, and 0.93% for x=0, 2, and 4, respectively. As a result, the higher the Ta content, the higher lattice strain in the β-Ti phase. The microstructures of the Ti–Fe–Ta alloys are presented in Figs. 1(b)–1(d). $Ti_{72}Fe_{28}$ [Fig. 1(b)] displays a hypoeutectic microstructure; β-Ti primary dendrites are embedded in an ultrafine (β-Ti+FeTi) eutectic matrix. The dendrite length (L), the primary (dendrite trunk) spacing (λ_1), and the secondary (dendrite arm) spacing (λ_2) of the

[a)]Author to whom correspondence should be addressed; electronic mails: lczhangimr@gmail.com and l.zhang@ifw-dresden.de

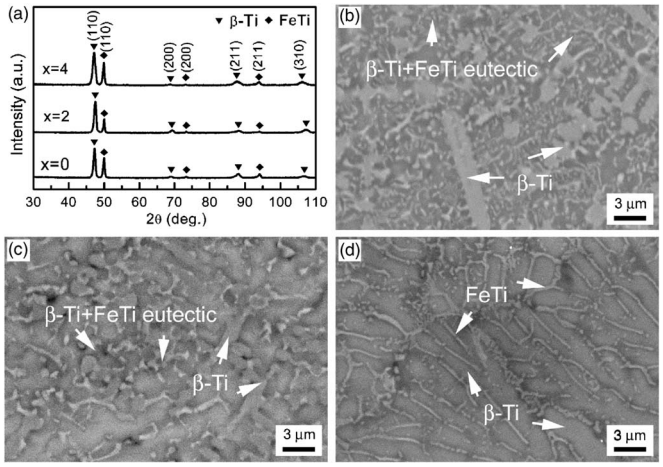

FIG. 1. (a) XRD patterns and SEM microstructures of the $(Ti_{0.72}Fe_{0.28})_{100-x}Ta_x$ alloys: (b) $x=0$, (c) $x=2$, and (d) $x=4$.

β-Ti dendrites are 10–30, 1–2, and 2–4 μm, respectively. The average width of the β-Ti and FeTi lamellae in the eutectic matrix is about 350 and 150 nm, respectively. The $Ti_{70.56}Fe_{27.44}Ta_2$ alloy has a similar microstructure as the Ta-free binary alloy [Fig. 1(c)]. The dendrite parameters (L, λ_1, and λ_2) of the primary β-Ti dendrites are 5–15, 1–2, and 2–5 μm, respectively. These values are similar to those for $Ti_{72}Fe_{28}$. However, this alloy has a significantly coarser eutectic matrix in comparison with $Ti_{72}Fe_{28}$. The average widths of the β-Ti and FeTi lamellae in the eutectic are about 1.0 μm and 400 nm, respectively, which are about three times coarser than in case of $Ti_{72}Fe_{28}$. In addition, according to the areal fractions in the microstructure, $Ti_{70.56}Fe_{27.44}Ta_2$ contains a smaller volume fraction of the ultrafine eutectic than $Ti_{72}Fe_{28}$. The $Ti_{69.12}Fe_{26.88}Ta_4$ alloy [Fig. 1(d)] has a different microstructure compared with the hypoeutectic structure in the former two alloys. It has a carcass microstructure composed of ultrafine FeTi (~250 nm) and micrometer-sized β-Ti (~1.2 μm) solid solutions.

Figure 2 displays TEM bright-field micrographs and the corresponding selected area electron diffraction (SAED) patterns of the UFG Ti–Fe–Ta alloys. The TEM observations

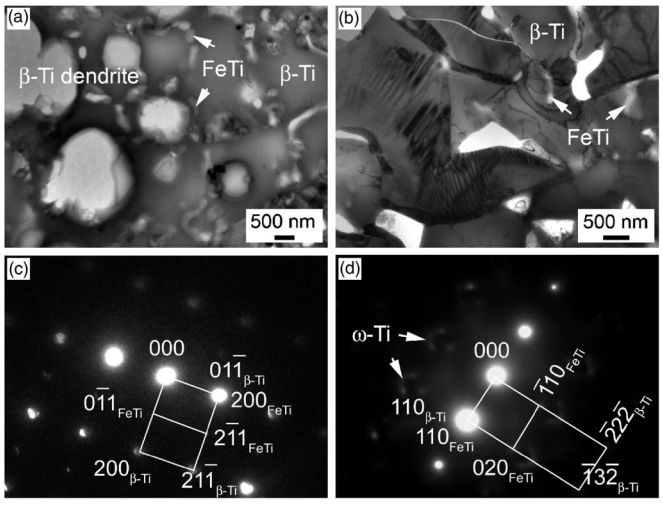

FIG. 2. Bright-filed TEM images of the ultrafine-grained $(Ti_{0.72}Fe_{0.28})_{100-x}Ta_x$ alloys, (a) $x=0$ and (b) $x=4$, and the corresponding SAED patterns for the eutectic matrix in (c) $x=0$ along the [011] zone axis and (d) $x=2$ along the [112] zone axis of the β-Ti phase.

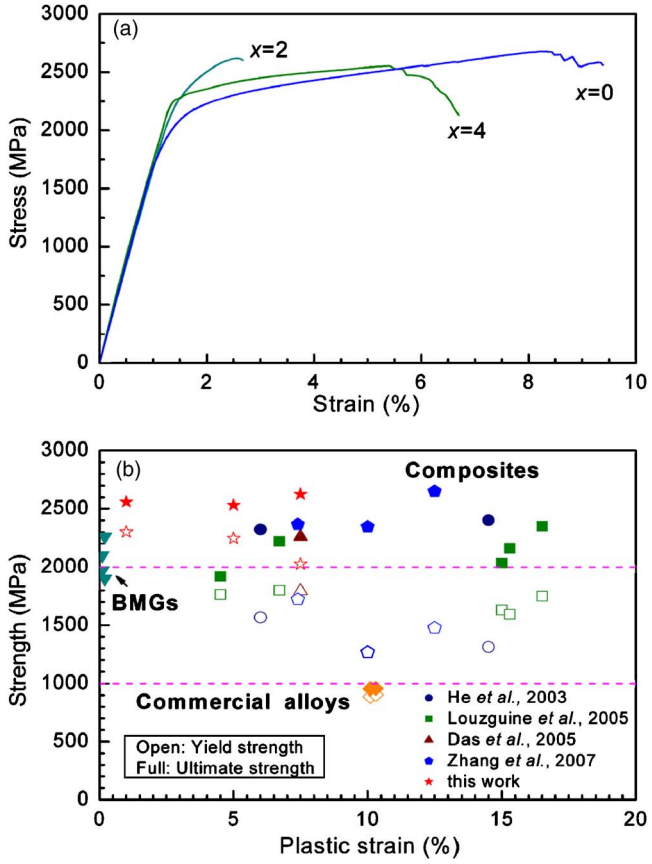

FIG. 3. (Color online) (a) Uniaxial compressive engineering stress-strain curves at room temperature for the ultrafine-grained $(Ti_{0.72}Fe_{0.28})_{100-x}Ta_x$ rods and (b) comparison of the mechanical properties of the present alloys with some Be-free Ti-based bulk metallic glasses (Refs. 4–7) and bimodal composites. (Refs. 14–17)

confirm that $Ti_{72}Fe_{28}$ [Fig. 2(a)] is composed of β-Ti primary dendrites embedded in an ultrafine (β-Ti+FeTi) eutectic matrix and the $x=2$ alloy displays a similar microstructure (not shown here), while $Ti_{69.12}Fe_{26.88}Ta_4$ [Fig. 2(b)] consists of nanoscale twins along with the β-Ti and FeTi phases. However, the SAED patterns reveal that the $x=0$ and $x=2$ alloys show different structural features in the matrix. The matrix of $Ti_{72}Fe_{28}$ displays only the diffraction spots of β-Ti and FeTi [Fig. 2(c)]. The two sets of spots are indexed as the diffraction patterns of the [011] zone axis of the β-Ti and FeTi phases. Their corresponding orientation relationships are $[011]_{\beta\text{-Ti}}\|[011]_{\text{FeTi}}$ and $(01\bar{1})_{\beta\text{-Ti}}\|(200)_{\text{FeTi}}$. In contrast, the matrix in $Ti_{70.56}Fe_{27.44}Ta_2$ [Fig. 2(d)] consists of a diffuse ω-Ti scattering (circular reflections around the FeTi diffraction spots) together with the diffraction spots of the β-Ti and FeTi phases. One set of the spots is indexed as the diffraction pattern of the $[\bar{1}12]$ zone axis of the β-Ti solid solution, and the other set corresponds to that of the [001] zone axis of FeTi. The corresponding orientation relationships between the β-Ti and FeTi phases are $[\bar{1}12]_{\beta\text{-Ti}}\|[001]_{\text{FeTi}}$ and $(110)_{\beta\text{-Ti}}\|(110)_{\text{FeTi}}$.

Figure 3(a) presents the room temperature uniaxial compressive engineering stress-strain curves of the UFG Ti–Fe–Ta alloys. The obtained mechanical properties are summarized in Table I. All alloys exhibit a high yield strength exceeding 2000 MPa, a high fracture strength over 2500 MPa, and a large plasticity over 5% except for the value of 1.0% found for the $Ti_{70.56}Fe_{27.44}Ta_2$ alloy. $Ti_{72}Fe_{28}$

TABLE I. Room temperature compressive mechanical properties for the $(Ti_{0.72}Fe_{0.28})_{100-x}Ta_x$ alloys: 0.2% offset yield stress $\sigma_{0.2}$, ultimate compressive stress σ_{max}, plastic strain ε_p, and fracture strain ε_f.

Ta content	$\sigma_{0.2}$ (MPa)	σ_{max} (MPa)	ε_p (%)	ε_f (%)
$x=0$	2028±20	2627±50	7.5±0.3	8.5±0.5
$x=2$	2300±11	2560±60	1.0±0.1	2.4±0.2
$x=4$	2215±6	2531±22	5.0±0.4	5.8±0.7

reaches a high yield strength of 2028 MPa, a fracture strength of 2627 MPa, and a plasticity of 7.5%. $Ti_{70.56}Fe_{27.44}Ta_2$ displays a lower plasticity and the $Ti_{69.12}Fe_{26.88}Ta_4$ alloy regains a large plasticity (Table I). It has been reported for other UFG Ti–Fe-based alloys that the refinement and the volume fraction of the phase constituents in the microstructure are crucial for their mechanical properties[17] and that the presence of short-range order (such as ω-Ti-like ordering in the β-Ti phase) and high lattice strain leads to a reduction of plasticity.[20] According to our XRD, SEM, and TEM results (Figs. 1 and 2), the addition of 2 at. % Ta results in a three times coarser and slightly lower volume fraction of eutectic matrix in $Ti_{70.56}Fe_{27.44}Ta_2$ compared with the $Ti_{72}Fe_{28}$ alloy. Moreover, the addition of 2 at. % Ta leads to the formation of the ω-Ti phase and 0.24% higher lattice strain for the β-Ti phase in this alloy compared to $Ti_{72}Fe_{28}$, which increases the pileup stress and decreases the intrinsic cleavage strength.[22] Therefore, the addition of 2 at. % Ta reduces the plasticity of the $Ti_{72}Fe_{28}$ alloy. On the other hand, it has been reported that deformation twinning enhances the plastic deformation in Ti-based alloys.[23] Thus, in the case of $Ti_{69.12}Fe_{26.88}Ta_4$, the presence of nanoscale twins inside the as-cast samples may facilitate the dislocation slip and enhance the plasticity. Further investigations are underway to fully understand the details of the deformation mechanisms for the different alloys. These results will be presented in a forthcoming paper.

Comparing the mechanical properties of the present UFG Ti–Fe–Ta alloys with some previously reported advanced titanium alloys [Fig. 3(b)], including Be-free Ti-based BMGs (Refs. 4–7) and Ti-based bimodal composites,[14–17] yields the following conclusions: compared with Ti-based BMGs, the UFG Ti–Fe–Ta alloys exhibit a slightly higher yield strength over 2000 MPa and a distinctly larger plasticity. They also show a slightly higher fracture strength and a similar plasticity but an appreciably higher yield strength when compared with the reported bimodal composites. With respect to the yield strength, the UFG Ti–Fe–Ta alloys exhibit 700–950 MPa higher yield strength than the $Ti_{60}Cu_{14}Ni_{22}Sn_4Nb_{10}$ alloy[14] and 200–1000 MPa higher yield strength than UFG Ti–Fe-based bimodal composites.[15–18] Altogether, the as-developed UFG Ti–Fe–Ta alloys exhibit not only a high fracture strength >2500 MPa but also a high yield strength >2000 MPa along with a plasticity of 5%–7.5%, which renders these alloys superior to high-strength Ti-based BMGs and bimodal composites. In addition, a low Ta concentration will not make these alloys expensive. These UFG Ti-based alloys are expected to exhibit even larger plasticity together with high strength after secondary processing to reduce casting flaws.[24]

The authors thank M. Frey, H.-J. Klauß, and S. Donath for technical assistance. One of the authors (L.C.Z.) is very grateful for the financial support of the Alexander von Humboldt Foundation.

[1] E. Ma, JOM **58**, 49 (2006).
[2] C. C. Koch, J. Metastable Nanocryst. Mater. **18**, 9 (2003).
[3] C. Leyens and M. Peters, *Titanium and Titanium Alloys: Fundamentals and Applications* (Wiley-VCH, Weinheim, 2003), p. 1–513.
[4] T. Zhang and A. Inoue, Mater. Sci. Eng., A **304-306**, 771 (2001).
[5] C. L. Ma, S. Ishihara, H. Soejima, N. Nishiyama, and A. Inoue, Mater. Trans. **45**, 1802 (2004).
[6] J. J. Oak, D. V. Louzguine-Luzgin, and A. Inoue, J. Mater. Res. **22**, 1346 (2007).
[7] Y. J. Huang, J. Shen, J. F. Sun, and X. B. Yu, J. Alloys Compd. **427**, 171 (2007).
[8] J. M. Park, H. J. Chang, K. H. Han, W. T. Kim, and D. H. Kim, Scr. Mater. **53**, 1 (2005).
[9] F. Q. Guo, S. J. Wang, S. J. Poon, and G. J. Shiflet, Appl. Phys. Lett. **86**, 091907 (2005).
[10] L. C. Zhang, J. Xu, and E. Ma, J. Mater. Res. **17**, 1743 (2002).
[11] L. C. Zhang, J. Xu, and J. Eckert, J. Appl. Phys. **100**, 033514 (2006).
[12] L. C. Zhang, Z. Q. Shen, and J. Xu, Mater. Sci. Eng., A **394**, 204 (2005).
[13] L. C. Zhang, J. Xu, and E. Ma, Mater. Sci. Eng., A **434**, 280 (2006).
[14] G. He, J. Eckert, W. Löser, and L. Schultz, Nat. Mater. **2**, 33 (2003).
[15] D. V. Louzguine, L. V. Louzguina, H. Kato, and A. Inoue, Acta Mater. **53**, 2009 (2005).
[16] J. Das, K. B. Kim, F. Baier, W. Löser, and J. Eckert, Appl. Phys. Lett. **87**, 161907 (2005).
[17] L. C. Zhang, J. Das, H. B. Lu, C. Duhamel, M. Calin, and J. Eckert, Scr. Mater. **57**, 101 (2007).
[18] D. V. Louzguine, H. Kato, L. V. Louzguina, and A. Inoue, J. Mater. Res. **19**, 3600 (2004).
[19] B. B. Sun, M. L. Sui, Y. M. Wang, G. He, J. Eckert, and E. Ma, Acta Mater. **54**, 1349 (2006).
[20] J. Das, J. Eckert, and R. Theissmann, Appl. Phys. Lett. **89**, 261917 (2006).
[21] T. Ohkubo, D. Nagahama, T. Mukai, and K. Hono, J. Mater. Res. **22**, 1406 (2007).
[22] P. Lazar, R. Podloucky, and D. Wolf, Appl. Phys. Lett. **87**, 261910 (2005).
[23] X. P. Wu, S. R. Kalidindi, C. Necker, and A. A. Salem, Acta Mater. **55**, 423 (2007).
[24] D. Jia, Y. M. Wang, K. T. Ramesh, E. Ma, Y. T. Zhu, and R. Z. Valiev, Appl. Phys. Lett. **79**, 611 (2001).